Geophys. J. Int. (1991) **105,** 85–102

Results of NFP 20 seismic reflection profiling along the Alpine section of the European Geotraverse (EGT)

P. Valasek,[1] St. Mueller,[1] W. Frei[2] and K. Holliger[1]

[1] *Institut für Geophysik, Eidgenössische Technische Hochschule (ETH), CH-8093 Zürich, Switzerland*
[2] *Programmleitung NFP 20, Feldeggweg 9, CH-8634 Hombrechtikon, Switzerland*

Accepted 1990 September 4. Received 1990 August 31; in original form 1990 May 3

SUMMARY

Recent deep-crustal seismic reflection profiling across the central Alps of eastern and southern Switzerland has provided a detailed image of this continental collision zone. As part of the Swiss National Science project NFP 20, a series of reflection profiles was recorded during two phases along N–S transects crossing the Alpine edifice. The eastern and southern profiles coincide with the Alpine segment of the European Geotraverse (EGT) and in part with the earlier Swiss Geotraverse. These data together with other geophysical and extensive geologic information form a unique and comprehensive volume of crustal information for this region of the Alps. On a larger scale, the new reflection data also add to a growing set of profiles crossing the Alpine fold belt which includes an additional traverse carried out by NFP 20 across the western Swiss Alps and the ECORS–CROP profile across the western Alps. The initial results of the reflection data across the central Alps outline a crustal framework involving northward indentation of the Adriatic hinterland into the subducting European foreland. This occurs beneath the collapsed oceanic basins of the Penninic allochthon which is defined by its highly reflective crystalline nappes. The present crustal thickness within the Alpine collision zone has doubled to about 60 km by both vertical and horizontal displacements along an inferred complex detachment system controlled by the Adriatic wedge. The south-plunging European foreland implies that portions of the thickened crust have been subducted into the upper mantle. This general framework of flake tectonics is laterally consistent with the ECORS–CROP results from the western Alps. However, the western Alps show a higher degree of crustal imbrication which may be related to the presence of the rigid Ivrea body and an overall greater amount of crustal shortening compared to the central Alps.

Key words: Alpine tectonics, crustal indentation, European Geotraverse (EGT), intracrustal detachment, lithospheric subduction, seismic reflection profiling.

1 INTRODUCTION

The Alps are part of a broad belt of deformation developed during the collision of the Eurasian and African lithospheric plates. Within Switzerland, the collision involved the convergence of the northernmost spur of the African plate, the Adriatic promontory or Apulian microplate, with the European part of the Eurasian plate. The relatively pristine state of this young orogenic zone makes it an ideal target for illuminating compressional tectonic features of the lithosphere. Over the years, various geoscientific investigations have been combined to produce an Alpine model which is characterized by an intensely imbricated upper crust and an overall asymmetric crustal thickness reaching to depths of 55–60 km (*cf.* Mueller *et al.* 1980). However, the low density of subsurface information available at the time provided only a limited resolution into many important crustal features. Currently, a new volume of information is emerging from renewed investigations along the central Alps. Led by the European Geotraverse (EGT, *cf.* Mueller & Banda 1983), new geophysical data, including dense seismic refraction measurements, have been collected across the Alpine arc (Fig. 1). At the same time, the Swiss National Science Foundation initiated a programme (NFP 20)

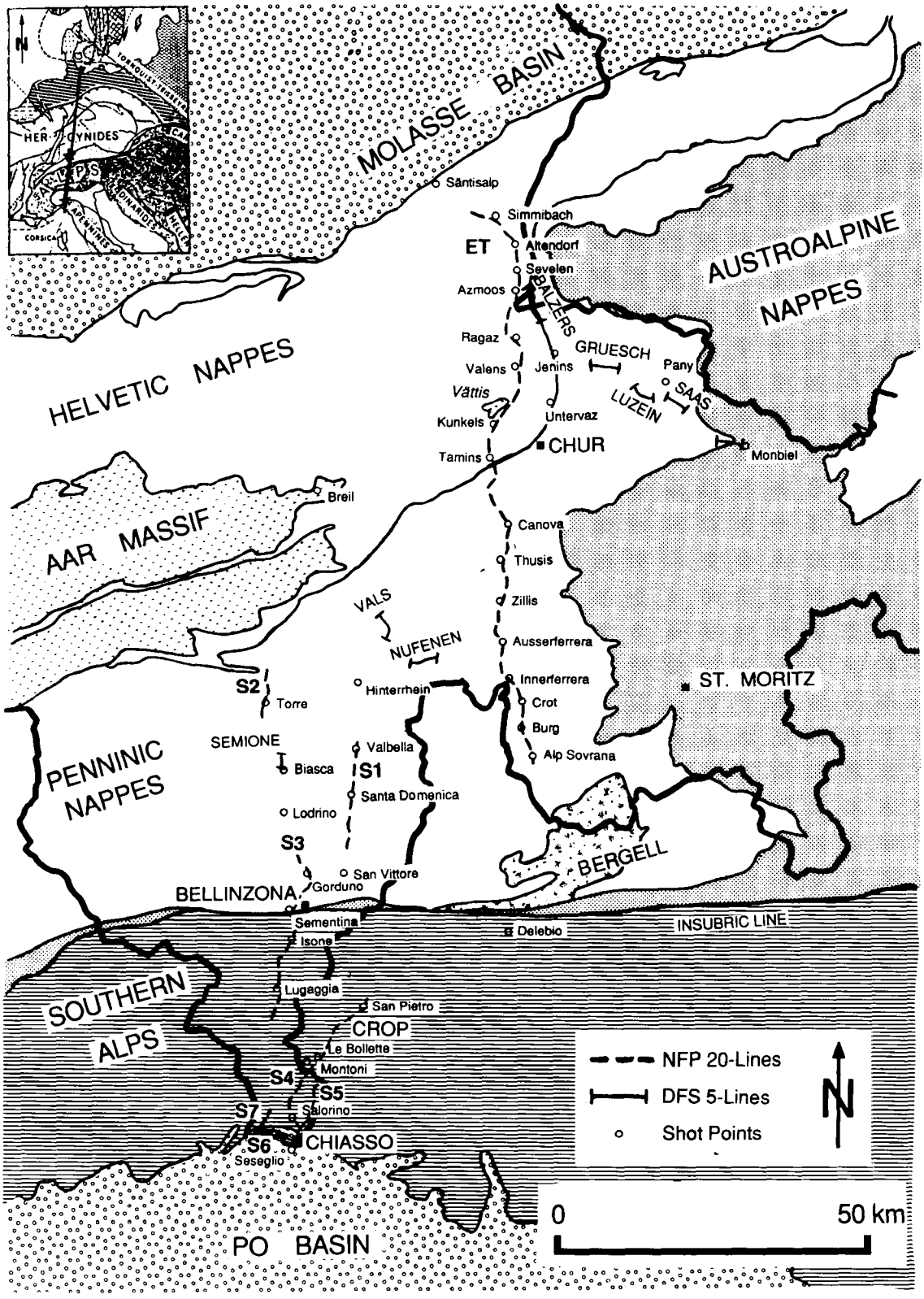

Figure 1. Location map and general tectonic setting of the NFP 20 eastern (ET) and southern traverse (lines S1–S7) seismic reflection profiles. Additional off-line recordings carried out by ETH Zürich are also indicated (DFS V lines). Measurements along and across the Italian border were undertaken in cooperation with CROP-Italia. The circles indicate sources of dynamite recordings. The inset shows the trace of the central and part of the southern segment of the European Geotraverse (EGT) (solid line). The heavy line indicates the Alpine section of the EGT between the shotpoints E and B2 (denoted by stars). The main Alpine traverses were recorded in separate phases during the years 1986–1988.

with primary emphasis on seismic reflection profiling (see e.g. Pfiffner *et al.* 1988; Frei *et al.* 1989). Since 1986, three traverses have been recorded totaling over 300 km across the Alps. In addition, a reversed refraction profile with narrow station spacing linked to the reflection profiles was recorded along strike as part of the NFP 20 programme (Maurer 1989). These new data provide high-resolution seismic information extending down to the crust–mantle boundary which should improve the existing Alpine models. This paper presents the initial tectonic implications of the new reflection data recorded in the central Alps.

2 GEOLOGIC AND GEOPHYSICAL SETTING

The central Alps of eastern Switzerland are divided from north to south into three major tectonic domains, the Helvetic, Penninic and Southern Alps (Fig. 1). These units document various stages of deformation and metamorphism developed during the Alpine orogeny (*cf.* Frey *et al.* 1974).

The Helvetic units formed the southern margin of the European continent during the Mesozoic and were displaced during the later stages of Alpine folding (Oligocene to late Miocene, *cf.* Trümpy 1980). The thin-skinned Helvetic nappes consist of detached cover sediments which now rest on both syn-tectonic Molasse sediments and the autochthonous basement cover in the north (Pfiffner 1985). Variscan-aged basement which formed the continental margin was uplifted during a more recent phase of deformation and developed into large-scale domes such as the 'external' Aar Massif. This massif is mainly exposed west of the eastern traverse but appears to plunge eastward beneath the transect as revealed by an exposed 'window' near Vättis (Fig. 1).

Further south, the Penninic zone consists of crystalline nappes which may have comprised several continental blocks intervening within the Tethys ocean prior to collision in the late Cretaceous (Trümpy 1980). These Hercynian basement-cored nappes exhibit deep-seated regional metamorphism with peak temperatures reaching 650 °C (Frey *et al.* 1980) developed during the Late Eocene to Early Oligocene (Hurford, Flisch & Jäger 1989). Most of the oceanic cover (schistose Bündnerschiefer including ophiolite sequences) has been stripped off and either piled up in front of the nappes or mobilized between them (Pfiffner *et al.* 1990a). At the south end of this zone, the Insubric Line separates the highly metamorphosed Penninic units in the north from the unmetamorphosed Southern Alps (Frey *et al.* 1974). The latter consist mainly of deformed Mesozoic sediments that once formed the margin of the Tethys ocean. South-vergent thrusting predominates in this unit which was transported northward several hundred kilometres during Alpine compression.

An extrapolated cross-section to the base of the crust shows schematically the presumed relationship between these tectonic units at depth (Fig. 2, after Trümpy 1985). The shallow structures are well known based on extensive surface mapping and projections using the eastward axial plunge. One of the most notable features is the overthrusting of the Penninic nappes on the external massifs

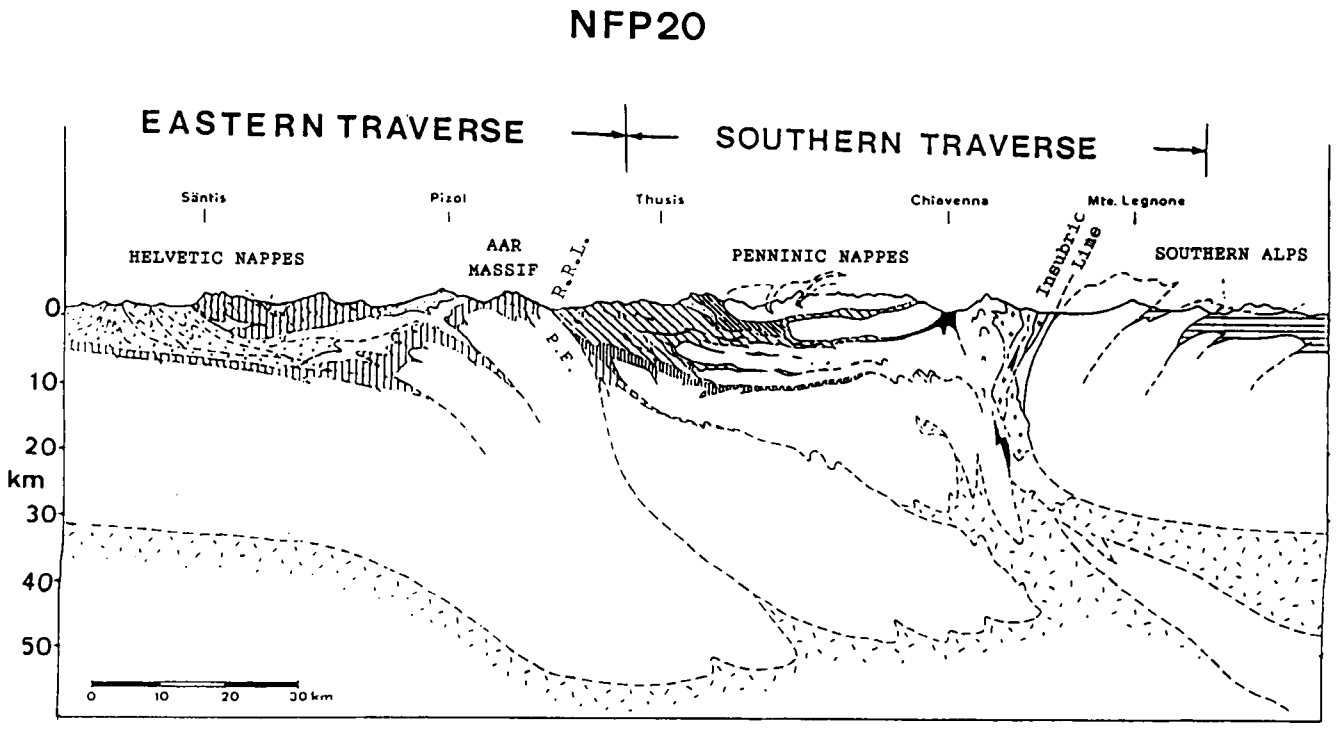

Figure 2. A schematic cross-section of the eastern Swiss Alps constructed prior to recording the NFP 20 seismic reflection data (Trümpy 1985). This profile shows the relationship, based on surface projections, of the main tectonic features: the Helvetic nappes, the Penninic nappes and the Southern Alps. The thrust and nappe style of deformation is clearly evident in the cross-section. Deeper in the section, the crust is shown to thicken beneath the Penninic allochthon. This geometry was constructed based on interpretations of earlier seismic refraction measurements (Mueller *et al.* 1980). R.R.L. = Rhine–Rhône Line, P.F. = Penninic Front.

(Pfiffner *et al.* 1990a). Estimates on the total amount of crustal shortening producing these thrust sheets varies between 400 and 500 km (Laubscher 1970, 1974; Dewey *et al.* 1973, 1989; Roeder 1989). These nappes are characterized by nearly horizontal penetrative plastic fabrics developed during their tectonic emplacement from deep crustal levels. In striking contrast, the crystalline massifs show much less Alpine overprint. Instead, they are characterized by predominantly vertical structures developed during the Variscan orogeny (Pfiffner *et al.* 1990a).

While the near-surface in Fig. 2 shows numerous details of the Alpine deformation, information at depths below 10 km is sparse. The limits of the crust–mantle boundary are based primarily on earlier seismic refraction measurements and gravimetric considerations (Mueller *et al.* 1980; Kissling, Mueller & Werner 1983). The Moho is shown to deepen considerably toward the crustal root zone to a depth of approximately 60 km compared to about 30 km in the adjacent regions outside the Alps. Important questions regarding the nature and evolution of the plate interactions during the collision, particularly within the crustal root zone, remain largely unanswered. Also, the extent and nature of the major intracrustal detachment zones at depth are not yet clear. The goals of the reflection experiments of NFP 20 were to provide a detailed image of the present crustal configuration and to shed light into questions regarding Alpine tectonics.

3 DATA ACQUISITION AND PROCESSING

Young mountain belts are ideal locations for studying relatively well-preserved tectonic features; however, they are logistically some of the most difficult areas to gather data from. Switzerland is no exception, numerous problems arise from recording seismic reflection data across its rugged mountains and densely populated valleys. Within the valleys, source and receiver coupling conditions can degrade severely and the ambient noise level is at a constant high level. In the quieter mountains, access is limited and the topographic changes across the geophone arrays can vary on the order of hundreds of metres creating significant static problems. These difficult recording conditions strongly influenced the design of the deep-crustal profiles planned by NFP 20.

In order to sample across the strike of the Alps, a compromise between recording in the mountains and in the valleys had to be made. This led to three generally north–south oriented transects. The eastern traverse (ET) and the southern traverse (lines S1 to S7) are depicted in Fig. 1, while the western traverse completed in 1987 is not shown. The first two of these three transects are discussed in this paper: the eastern traverse recorded in 1986 and portions of the southern traverse along which data were collected in seven segments in 1988 with cooperation of CROP-Italia. These profiles coincide with the Alpine section of the EGT.

To provide information from the near-surface down to the Moho, signals from two types of sources, Vibroseis and dynamite explosions, were recorded along the NFP 20 transects. Recordings were made primarily during the night-time periods when the traffic density, and therefore, the ambient noise level, was at a minimum. The dense Swiss transportation network, in particular the electric railway system ($16\frac{2}{3}$ Hz), produces high noise levels which are difficult to avoid.

Table 1. General acquisition parameters designed for the NFP 20 seismic reflection traverses. Both dynamite and Vibroseis were used as sources to provide two data sets for each traverse. Average charges of 100 kg detonated every 5 to 10 km provided sufficient deep-crustal reflection data. Denser Vibroseis measurements provided a high-resolution sampling of shallower structures. Most of the data were recorded using a 240 channel SERCEL SN 348 telemetric system. Recording was carried out by Prakla–Seismos for the eastern and southern traverses. Additional recordings were made using a 48 channel DFS V system operated by the ETH Zürich.

Dynamite	
Spread length	19.12 km
Group interval	80 m
Number of geophones/group	18-24, in-line
Source interval (approximate)	5 km
Average charge size	100 kg
Record length	60 s
Field filter (optional)	50 Hz
Sampling rate	4 ms
Nominal fold	1-4
Vibroseis	
Spread length	19.12 km
Group interval	80 m
Number of geophones/group	18-24, in-line
Number of vibrators	5-6
Source interval	40 m
Sweep frequencies	10-48 Hz
Sweep length	60 s (20 s)
Recording length	64 s (40 s)
Number of sweeps/VP	1-4
Sampling rate	4 ms
Nominal fold	120

Details of the recording parameters for the surveys are summarized in Table 1. A long receiver spread (19.12 km) enabled undershooting of some of the near-surface complexities and provided sufficient moveout for distinguishing deeper events based on velocity. The split-spread receiver configuration ensured continuous up-dip recording within the complex structures.

The use of vibrators as the primary source led to high-resolution coverage of the upper crust. A special 60 s long sweep was designed which provided superior results by supplying more energy compared to shorter, more conventional sweeps (1.7 times more energy compared to a 20 s sweep, *cf.* Stanley 1986). Recording primarily uncorrelated and unsummed records enabled additional pre-correlation and pre-summation signal-to-noise (S/N) enhancement techniques to be applied in the processing centre (*cf.* Coruh & Costain 1983).

Dynamite recordings provided at least single-fold coverage along the profiles yielding broad-band information powerful enough to penetrate down to deep crustal levels. At some localities, broadside shots were recorded to give information on the lateral continuation of structures. Additional off-line recordings of the larger explosions were

provided by a 5 km long spread operated by a team from the ETH Zürich.

Data processing is performed at a processing centre established by the NFP 20 program at the ETH in Zürich. The data presented here were processed following the flow chart outlined in Fig. 3. Two separate sequences were necessary to handle the two types of data, Vibroseis and dynamite, that were recorded. Processing of the low-fold dynamite data required fewer steps because of its smaller size compared to the multifold (up to 240 fold) Vibroseis data. Within 2 to 3 months following acquisition, the dynamite data were assembled into approximately single-fold common mid-point (CMP) sections. This data provided an early framework for processing and interpreting the Vibroseis data.

One of the primary objectives of data processing is to improve the S/N ratio. This was especially important for the Vibroseis data because of the unusually low S/N ratio resulting from the difficult recording conditions and the high degree of structural complexity. In particular, the data processing had to be designed to compensate for the variable coupling conditions, high ambient noise level and statics introduced during the data acquisition. To overcome these problems and to recover both shallow and lower amplitude deep events, special steps needed to be taken. Several iterations of velocity analysis following residual statics combined with spectral balancing, offset-limited stacking and coherency filtering were especially instrumental in achieving improved Vibroseis data quality (Valasek *et al.* 1990).

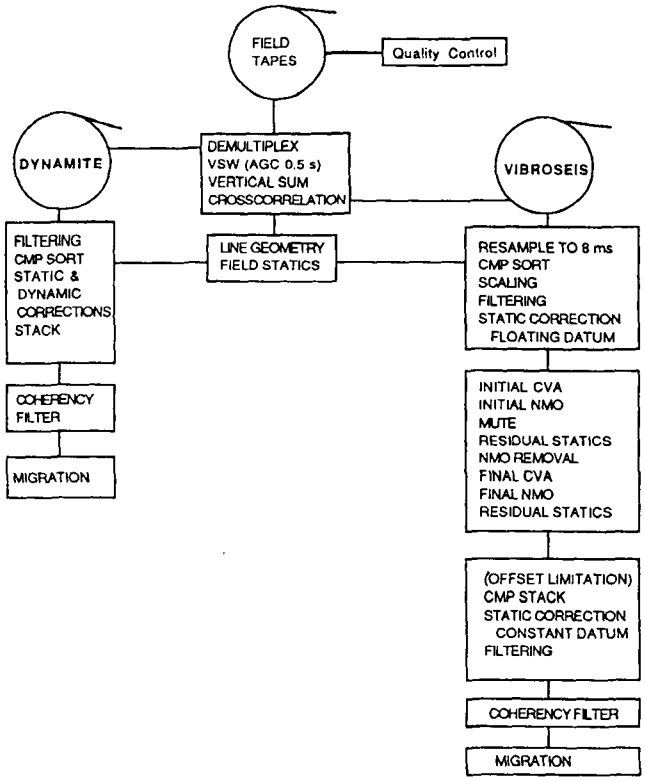

Figure 3. General processing structure used by the Zürich data centre for the NFP 20 seismic reflection traverses. An important feature of the data processing was the two sequences required for the two data types recorded: Vibroseis and dynamite. Early processing of the dynamite data provided a useful format for the more detailed processing of the Vibroseis data.

Offset-limited stacking helped to enhance the data quality in various problematic areas. Fig. 4 shows the effect of using only the near offsets (0 to 5 km) shot in the up-dip direction compared to the full-offset range (0 to about 20 km) on deep reflections recorded from the northern end of the eastern traverse. Near CDP 375, the profile crosses a wide valley which contains a major 'triple' junction for auto and rail networks. An improved image was realized by stacking only the focused data recorded near the source, thus eliminating far-offset traces characterized by low-amplitude, defocused (down-dip) energy. This was particularly helpful for enhancing the reflections recorded between CDPs 175 and 375 where the far-offset traces were either recorded in, or shot from within the noisy valley.

4 RESULTS

The seismic data are shown unmigrated in an automatic line drawing format at a 1:1 scale. The line drawing appearance of these sections was achieved by plotting only the strongest positive amplitudes following coherency filtering. Fig. 5 shows the results of both Vibroseis and dynamite recordings along the eastern traverse. In Fig. 6, the southern traverse profiles (S1, S3, S4, S5 in Fig. 1) are shown in a collage form using only the results of the dynamite recordings. Although the eastern and southern traverses form a continuous profile in the N–S direction, they are shown in two separate figures to emphasize their lateral E–W separation of approximately 25 km.

Upper crust

The upper levels of the crust are well defined on the Vibroseis section of the eastern traverse (Fig. 5a). The southern traverse also shows significant shallow reflectivity despite the poorer spatial resolution of the dynamite survey (Fig. 6). In the northern part of the eastern traverse (Fig. 5a), the data reveal a sequence of prominent reflectors (H) within the Helvetic domain. The basal reflection extends down to 3 s in the north and gradually climbs towards the south reaching the surface near the 'Vättis window' of the Aar Massif (*cf.* Fig. 1).

A transparent zone is observed beneath this wedge which continues from the surface south of Vättis until near Tamins where a well-defined wedge of reflections (P) emerges within the Penninic domain. This region is dominated by packages of subhorizontal, multicyclic reflections which reach down to approximately 5 s beneath Ausserferrera where they begin to bottom out and continue to the southern edge of the section.

Along the southern traverse (Fig. 6) another package of reflectors (P) is observed below the structurally deeper Penninic units exposed in this region. These reflections continue to the south uninterrupted until Santa Domenica where a prominent, north-dipping reflector is observed reaching from 6 s in the north up to almost 3 s in the south.

Further to the south, the data reveal sparse reflectors which are characterized by a northern dip. Most notable are the subparallel reflections between Isone and Lugaggia between 2–3 s and 4–5 s. At the southernmost end of the

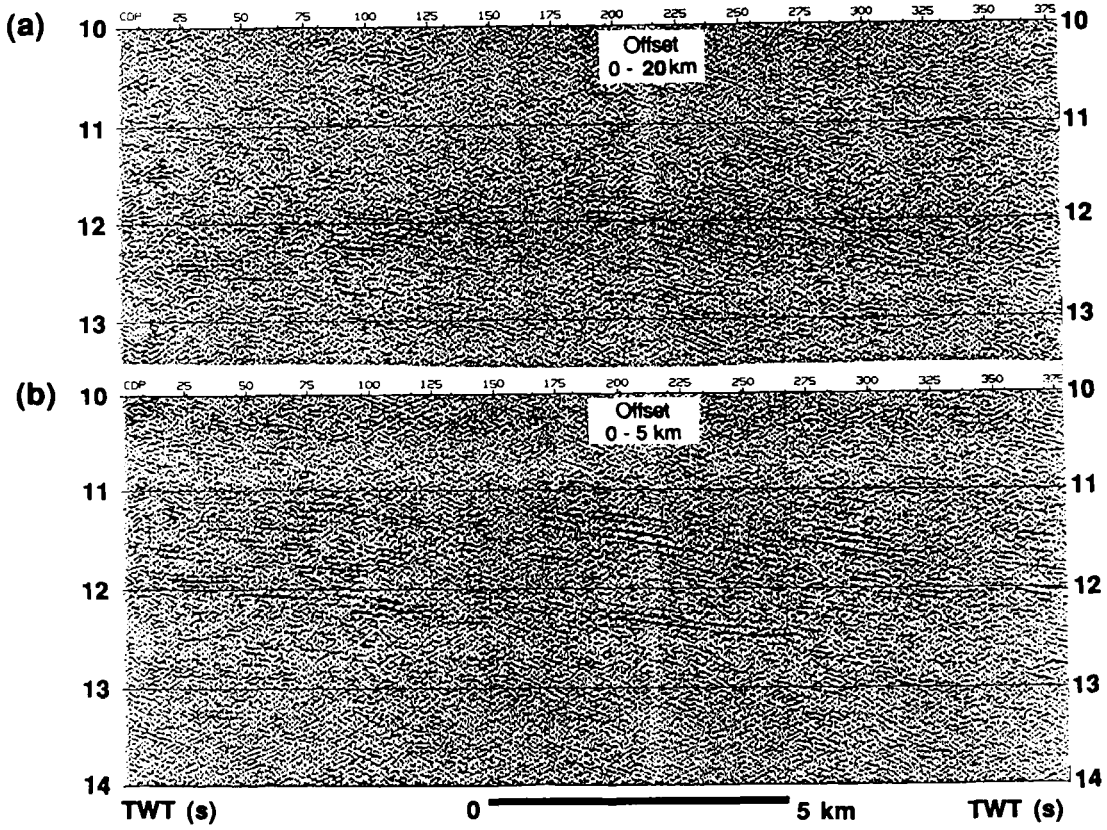

Figure 4. (a) A portion of the Vibroseis data from the northern end of the eastern traverse generated by using the full offset range from 0 to about 20 km for stacking. Deep reflections can be faintly seen between 11 and 13 s. A much clearer image is shown in (b) by stacking only the near traces with offsets less than 5 km recorded in the up-dip direction. The offset dependency of the stack quality was noticed in several areas across the Alps. This phenomenon is best explained by destructive interference of data with low signal-to-noise ratio developed in areas characterized by high ambient noise and/or by near-surface anomalies.

traverse, a pronounced horizontal reflector is recognized between 4 and 5s.

Deep crust

The reflectivity of the deeper levels of the Alpine crust is dominated by the bright package of reflections (M1) beginning at 11 s in the north which dip towards the south (Fig. 5). Above this zone, however, the data show a significant decrease in the observed number of reflections. This area shows only the background of incoherent noise which is found on all of the seismic sections. Within this rather transparent region, several regions of weak reflectivity can be distinguished on both the Vibroseis and dynamite sections. One area consists of discontinuous reflections between 6 and 8 s located beneath the 'Vättis window' of the Aar Massif. Another region is more clearly recognized dipping south between 8 and 9 s (L1) at the northern end of the traverse.

Undoubtedly, one of the most striking features of the eastern traverse is the high-amplitude package of south-dipping reflections (M1) beginning at 11 s (Fig. 5). This band of reflections, with a duration of approximately 1 s, continues uninterrupted southward until Thusis where its trace is lost at approximately 16 s. Interestingly, the southernmost extent of this event is slightly better defined on the Vibroseis section (Fig. 5a, beneath Thusis at 15 to 16 s) than on the dynamite profile (Fig. 5b). The unsuccessful imaging of the Moho in this region using explosions might be related to defocusing effects caused by shooting downdip compared to the split-spread Vibroseis configuration. Subhorizontal reflections are again observed on the southern end of the eastern traverse between 14 and 15 s. In addition, a series of north-dipping reflections can be seen cutting across these events.

Off-line measurements, including both in-line and fan recordings of dynamite shots, sample the eastern continuation of this deep boundary. Fig. 7 shows the fans recorded from the shot points Pany (a) and Monbiel (b) (*cf.* Fig. 1). The deep reflection packages between 12 and 16 s (M1) dip to the south and document the lateral continuity of the findings made along the eastern traverse. In addition, the deeper location of these reflectors (M1) indicates that this surface has an eastward component of dip.

Data from the southern traverse present a much different reflection pattern, especially south of the Insubric Line. Here the most notable feature at deeper levels is the strong band of energy (L2) dipping north from 7 s in the south to about 9 s at the northern end (Fig. 6). Additional in-line recordings measured north of the profile S1 (Fig. 8) reveal that this feature continues to dip north to around 13 s between Vals and Breil (*cf.* Fig. 1). Below this package of discontinuous reflections, a weaker set of subhorizontal reflections (M2) can be traced across profiles S3 and S5 between 12 and 14 s (Fig. 6). The remaining levels of the southern profile are transparent with the exception of the

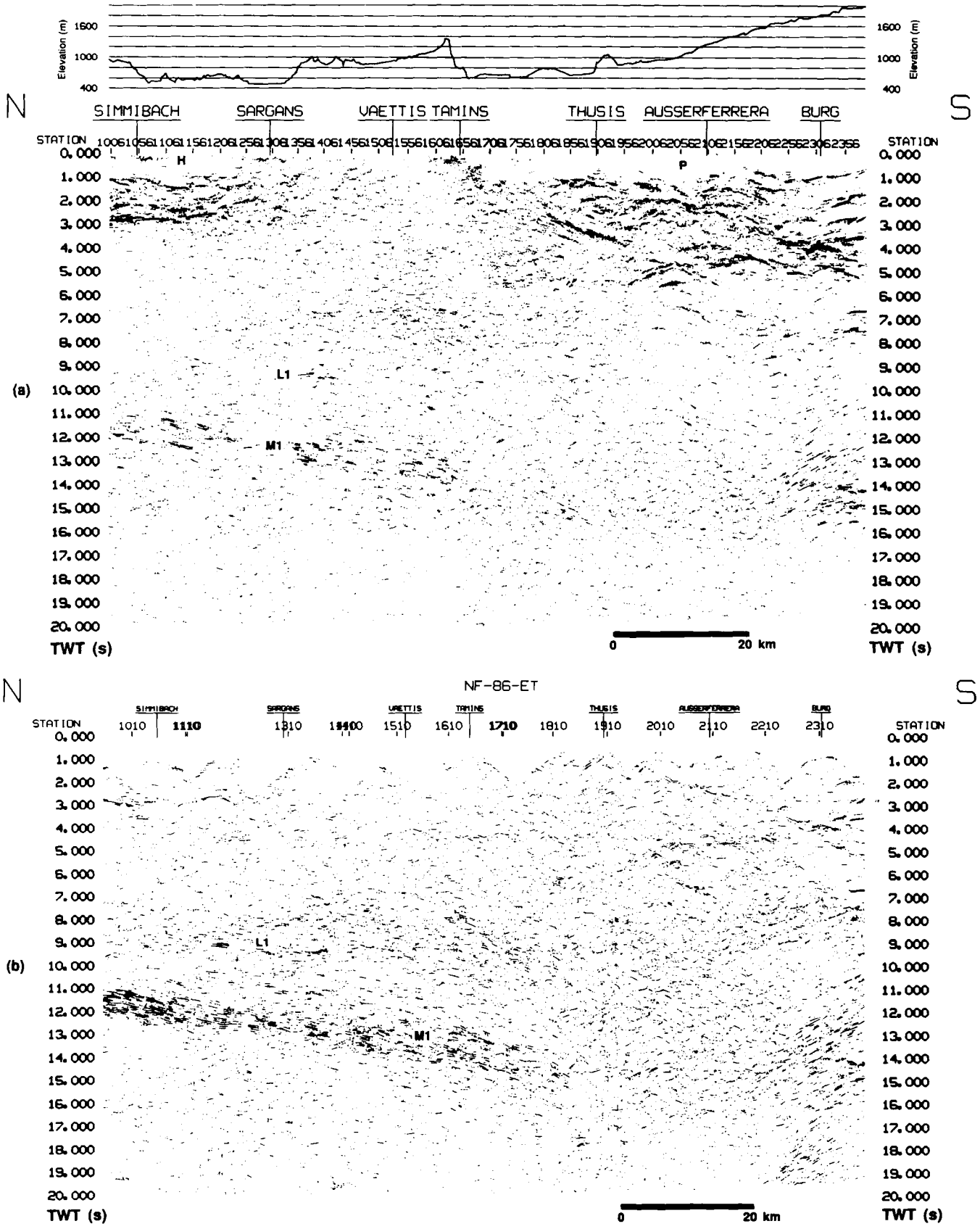

Figure 5. Results of the eastern traverse (*cf.* Fig. 1) obtained from (a) multifold Vibroseis measurements and (b) single-fold dynamite soundings. The Vibroseis data provided a high-resolution image of the shallow levels compared to the dynamite data. In contrast, the dynamite data provided much more prominent deep crustal information. This valuable complementary relationship between the two sources was a key to the success of the NFP 20 experiment. The labelled reflections are discussed in detail in the text.

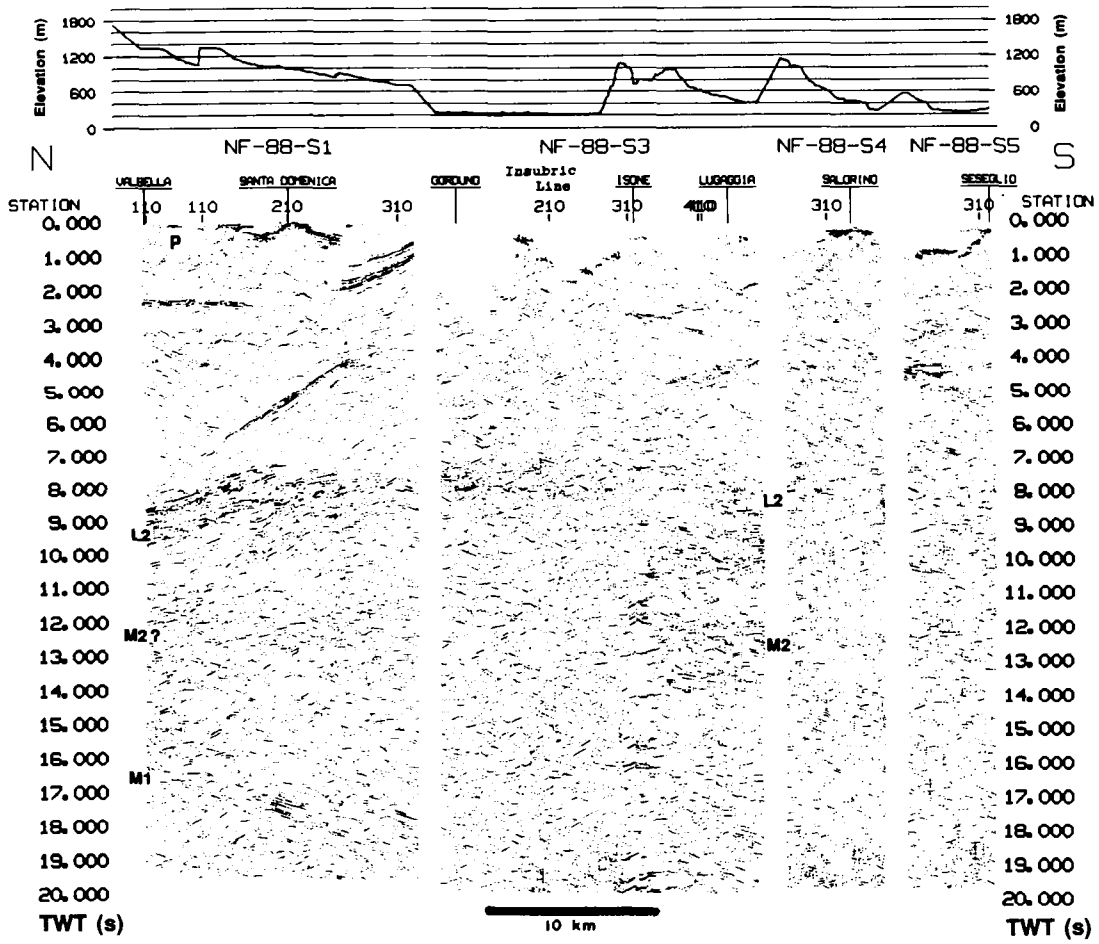

Figure 6. Results of the southern traverse (*cf.* Fig. 1) recorded from dynamite sources only. Sections from lines S1, S3, S4 and S5 only are shown. The labelled reflections are discussed in detail in the text. The vertical strip beneath Isone in the Middle of the line S3 is contaminated by noise from a powerful radio transmitter. The sections are displayed in approximately their true spatial locations.

deep, south-dipping reflections (M1) between 17 and 19 s on the northern end of the profile S1.

EGT wide-angle reflection data

The EGT refraction data across the Alps and adjacent regions are currently being investigated to obtain detailed information on the velocity structure (Ye & Ansorge 1990; Buness *et al.* 1990). In Fig. 9, we show the actual data processed in a format similar to the deep-crustal reflection data of NFP 20. This north–south section stretches from the northern margin of the Molasse Basin (shotpoint E) across the Alps and into the Po Basin (shotpoint B2) (Fig. 1, inset). Processing of the EGT refraction data was designed to enhance primarily the *PmP* wide-angle reflected phase. Information from a total of four shots (E, D. C and B2) were used which were recorded from offsets up to 290 km using an average receiver spacing of 2.5 km. To generate the display, the data were sorted according to their mid-point locations, shifted to a constant datum (700 m), NMO corrected and muted to remove the refracted phases. By using a realistic average crustal velocity (6.1 km s^{-1}, *cf.* EUGEMI Working Group 1990), the hyperbolic NMO correction holds for the large range of offsets used to record the refraction data. The influence of the general Moho topography on the traveltimes (Mueller *et al.* 1980) was also taken into account. Because the frequency and amplitude varied strongly with offset, the envelope was calculated to produce a more uniform image. The resulting image reproduces the general 'topography' of the *PmP* phase across the Alps and into adjacent regions. Similar processing of refraction data has been recently applied to data from the Canadian Shield (Mereu 1990) and routinely to fan recordings (e.g. in the western Alps, Hirn *et al.* 1989).

A major advantage of displaying the EGT data in this fashion, as opposed to the conventional reduced traveltime format, is that it allows a direct integration with the NFP 20 reflection data. To demonstrate this, portions of the NFP 20 data have been superimposed onto this section (Fig. 9a). The data were projected east–west along the Ivrea-corrected gravity isolines (Kissling *et al.* 1983) after assuming that the deep structures were laterally continuous over distances limited to a few tens of kilometres (*cf.* western Alps, Hirn *et al.* 1989). The increased intracrustal resolution of the NFP 20 data together with the illumination of the overall crustal structure provided by the EGT refraction measurements form an important data base for interpretation.

In Fig. 9, the onset of the high-amplitude *PmP* wide-angle phases coincides with the base of the near-vertical incident

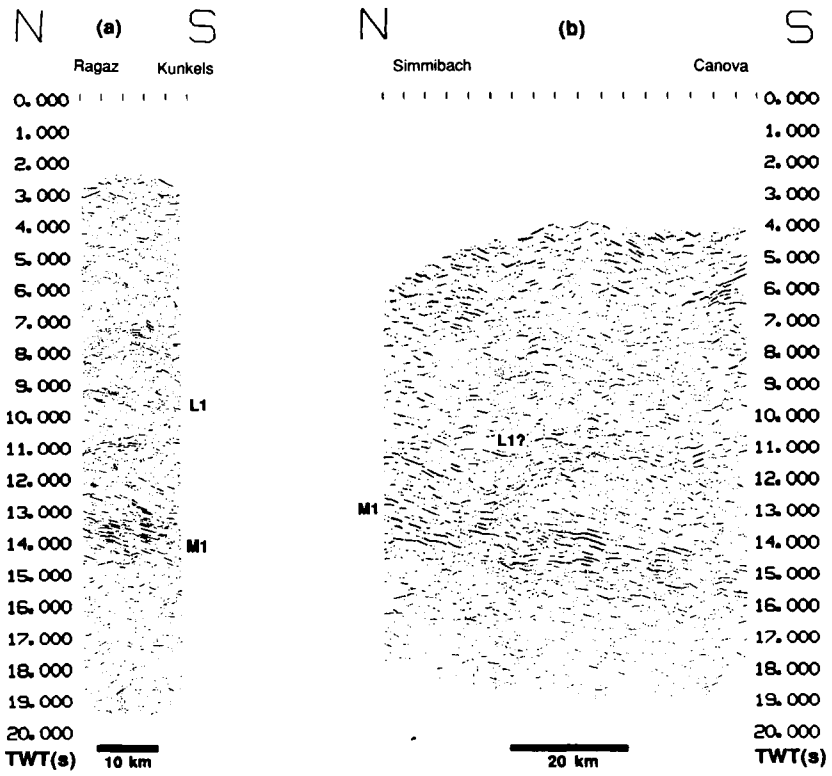

Figure 7. Off-line recordings measured east of the eastern traverse near Chur (*cf.* Fig. 1). (a) Fan recording from shot point Pany into 240 channels (20 km) spread out from north of Ragaz to Kunkels. (b) Fan recording from the shotpoint Monbiel into receivers extending approximately 70 km from the northern end of the eastern traverse (Simmibach) down to a location between Canova and Thusis. Both shots have had normal moveout (NMO) applied. The subsurface sampling is located in a position trending halfway between the shots and the recording spreads.

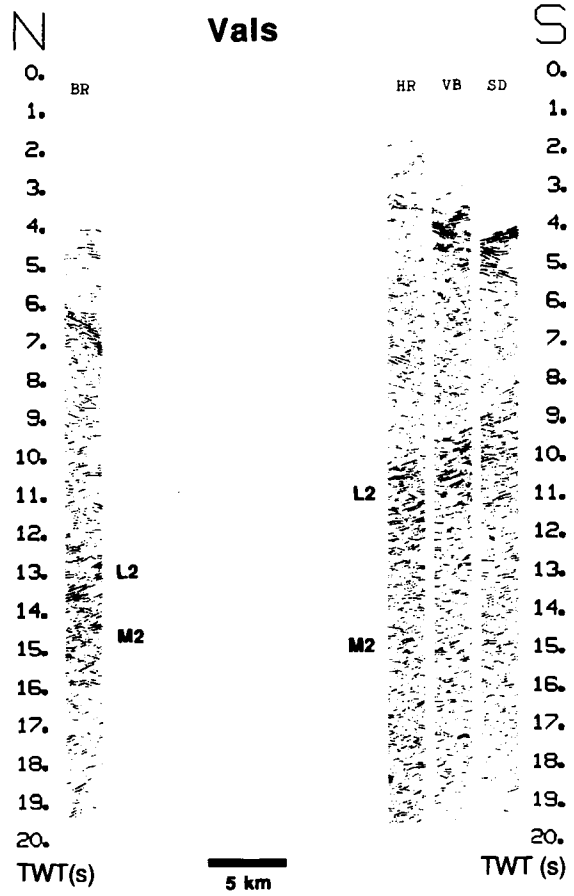

reflection zones M1 and M2 identified on the NFP 20 data (Figs 5 and 6). This correlation is superimposed on the composite section (Fig. 9b) and is also shown following migration (Fig. 9c). This relationship between near-vertical incidence and wide-angle reflections has been reported in other areas such as the Basin and Range province of North America (Klemperer *et al.* 1986) and in the North Sea (Barton 1986). The reflection M1 dips gently from about 9 s south of shotpoint E in the north until a location near shotpoint D where it plunges downward beneath profile S5 to around 23 s. From south to north, phase M2 is recognized at around 11 s beneath the Po Basin and bends down northward to about 16 s beneath shotpoint C at the Insubric Line. The variable character of the *PmP* phase is a function of the recording offsets. Data received from the larger, post-critical ranges (>90 km), such as beneath the Molasse Basin and the Po Basin, show the usual large increase in energy compared to the pre-critical distances. The implications of these two combined data sets will be discussed in the following sections.

Figure 8. A collage of four shots recorded by the DFS V spread Vals located north of profile S1 (*cf.* Fig. 1). From north to south the shots Breil (BR), Hinterrhein (HR), Valbella (VB) and Santa Domenica (SD) were recorded into the 5 km long DFS V spread. These data show the northern extension of the reflection package L2 located between 7 and 9 s on line S1 (Fig. 6). The subsurface sampling is located in a position centred halfway between the shots and the recording spread Vals.

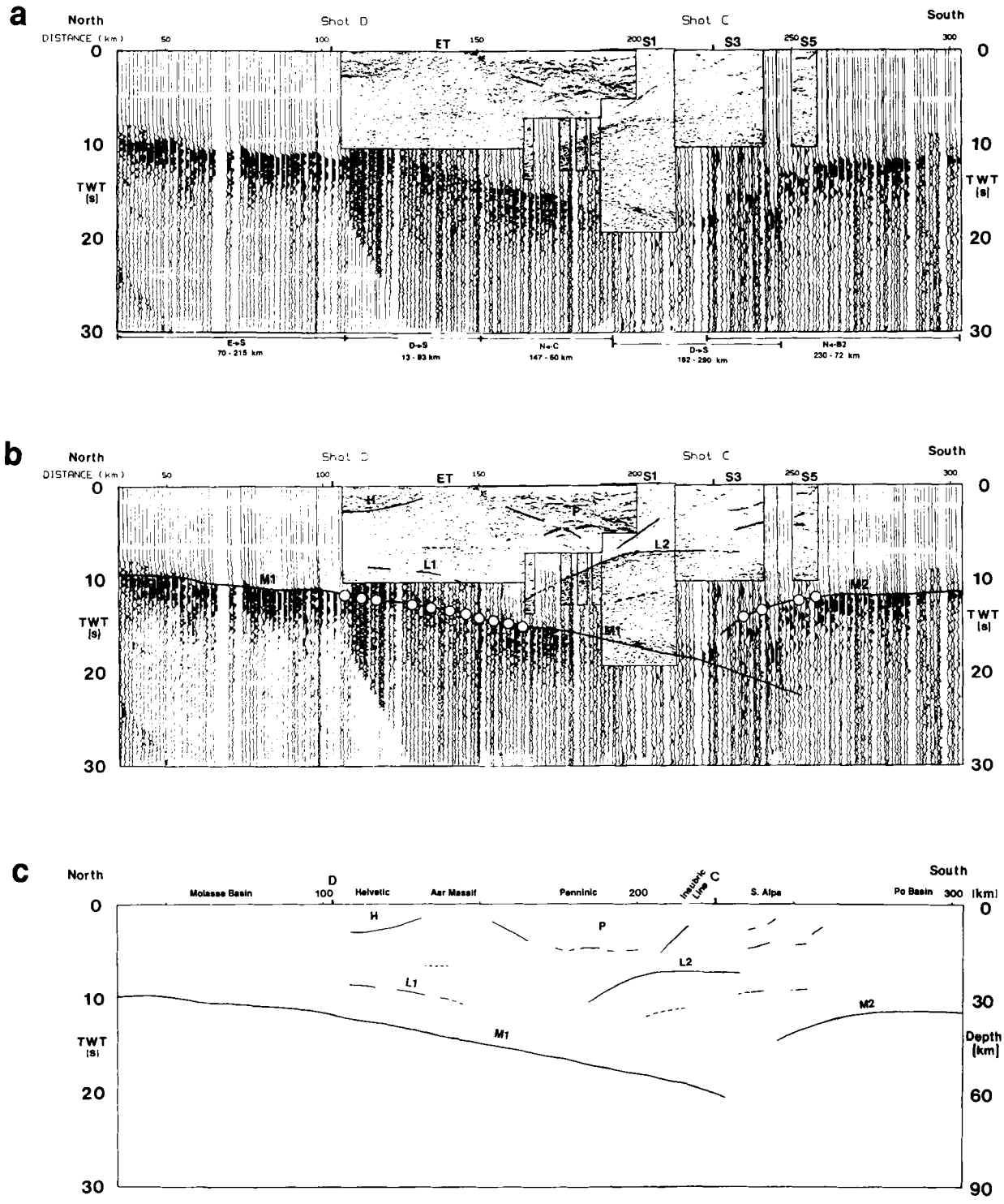

Figure 9. (a) Composite section of the EGT seismic refraction data across the Alps and Po Basin (inset, Fig. 1) and the NFP 20 reflection data. Refer to text for a detailed explanation of this display. The offsets used from the four EGT refraction shots are shown below the section (e.g. E→S translates to shot E recorded to the south). The distance scale above the profile is measured from EGT shot E. Shot B2 is located 37 km off the southern end of the profile. The four narrow strips located beneath line ET and north of line S1 are the off-line recordings (Vals) shown in Fig. 8. (b) Correlation of the main crustal boundaries. The white circles represent the superposition of the base of the crustal plates M1 and M2 obtained from the near-vertical incidence recordings (Figs 5 and 6). (c) 2-D hand migration of the main crustal boundaries shown in (b). A velocity of 6.1 km s^{-1} was used to reposition the reflections to their true subsurface origins.

5 INTERPRETATION

Helvetic and Penninic domains

The high resolution of the near-vertical incidence reflection data outlines important relationships of the ongoing Alpine deformation. Interpretation of the upper crustal reflections relies on the ability to correlate the seismic data to well-known geologic structures exposed on the surface. This provides the necessary geometric constraints for defining the thrust and nappe tectonics which dominates the shallow levels of the Alpine crust. At this stage only the general features of the upper crust will be addressed. A first interpretation of the explosion seismology results of NFP 20 has been given by Pfiffner *et al.* (1988) and a more detailed interpretation based on the Vibroseis data is discussed by Pfiffner *et al.* (1990b) and by Stäuble (1990).

In the northern Helvetic domain (H), the base of the Säntis nappe is recognized between 1.0 and 1.5 s thrust over the Molasse sediments and the Mesozoic–Cainozoic cover of the Variscan basement (Fig. 5a). The bright reflection at 3 s marks the top of the Mesozoic sediments. The autochthonous basement below the Helvetic zone is largely devoid of reflections. A similar non-reflective seismic expression is recognized across the outcrops of the Aar Massif. This external massif consists of near-vertical structures which may explain its poor seismic response.

The reflection character of the Helvetic domain is shown enlarged in Fig. 10. The reflections previously discussed show a sharp character that varies in continuity from a few tens of metres to several kilometres. In contrast, the Penninic reflections in the south appear more multicyclic and discontinuous with apparent dips to both the north and the south (Fig. 11). These distinctive reflection signatures may be related to the different internal properties of the (crystalline) Penninic and the (calcareous) Helvetic thrust sheets. In the north, the units underwent anchizonal to lower greenschist facies metamorphism compared to the upper greenschist- to amphibolite-grade metamorphism experienced in the Penninic units (Frey *et al.* 1980). This lower grade of metamorphism observed in the north combined with a 'low frequency' of compositional variations may account for the observed sharp reflectors. In the oceanic and continental rocks of the Penninic domain, deep-seated deformation produced an overall gneissic fabric which grades to mylonitic foliation in some areas. These typically planar, layered, anisotropic structures have been suggested to produce strong multicyclic reflections through constructive interference (Fountain, Hurich & Smithson 1984; Hurich & Smithson 1987). Mylonitic zones have been shown to be detectable reflectors in field measurements in other areas, such as the compressional belt of the Southern Appalachians (Christensen & Szymanski 1988) and in the metamorphic core complex belt of western North America

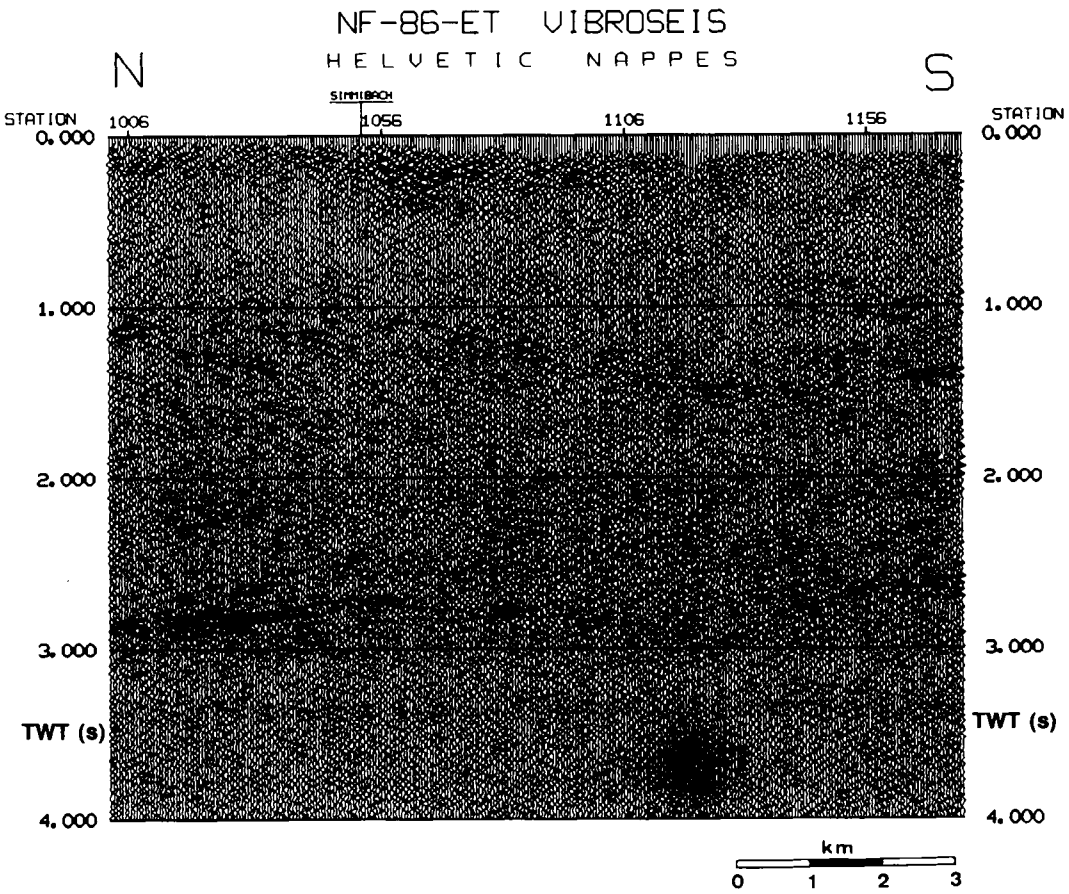

Figure 10. Enlargement of the northernmost window of the eastern traverse Vibroseis section (Fig. 5a) showing the details of the Helvetic nappe structures. The reflections are interpreted as representing primarily lithologic boundaries. This reflection response should be compared to the seismic expression recorded within the Penninic complex (Fig. 11).

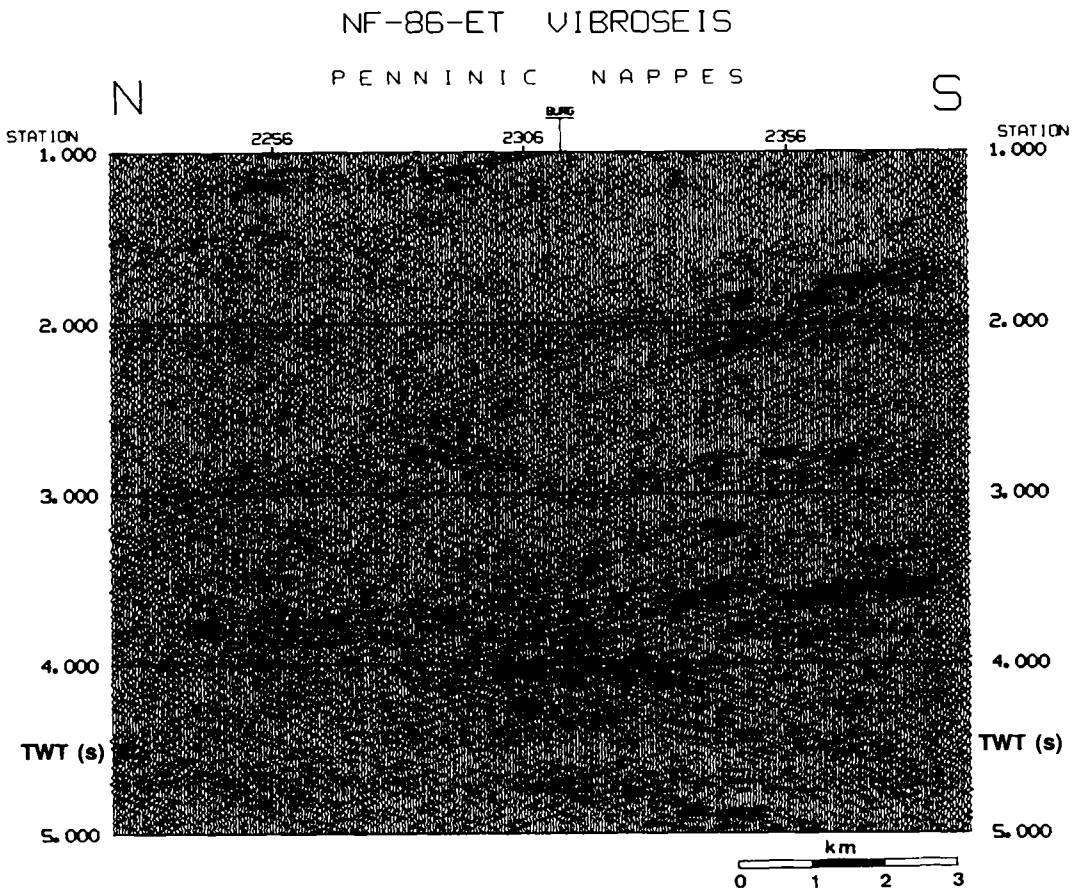

Figure 11. Enlargement of the southernmost window of the eastern traverse Vibroseis section (Fig. 5a) showing the details of the Penninic nappe structures. The high-amplitude, multicyclic reflections are interpreted as being largely controlled by the planar layering of these gneissic to mylonitic units. Compare this response to the less-metamorphosed Helvetic nappes in Fig. 10.

(Hurich *et al.* 1985; Valasek *et al.* 1989). The reflection pattern observed in these regions has similarities to the system of reflections recognized in the Penninic domain suggesting that planar multidimensional layering induced by plastic flow together with compositional variations is largely controlling the nature of these reflectors.

The internal structure of the Penninic nappe complex (Fig. 11) indicates that the stacking of nappes observed on the surface is preserved at depth. The reflections can be correlated to individual nappes exposed on the surface by projecting the east-plunging outcrops into the seismic profile (Pfiffner *et al.* 1988, 1990b). From the seismic data, the entire sequence of nappes and Bündnerschiefer is separated by a detachment termed the 'Penninic Front' (P.F. in Fig. 2), which emerges as the Rhine–Rhône Line at the surface on the southern flank of the Aar Massif near Tamins (Fig. 5a).

To the west along the northern end of the southern traverse, a structurally deeper sequence of Penninic nappes (P) is exposed. The horizontal reflections at 2 s recognized on the seismic section S1 (Fig. 6) indicate that the nappe pile remains subhorizontal even at its deepest levels. These nappes possibly correspond to reflections observed at the base of the nappe sequence imaged between 3 and 5 s on the eastern traverse (Fig. 5a).

Insubric Line and Southern Alps

The entire Penninic package is bordered in the south by a major dextral strike–slip fault, the Insubric Line (Figs 1 and 2). This Late Oligocene feature has been postulated to be a deep-reaching fracture zone with significant implications for Alpine deformation (Gansser 1968; Laubscher 1970). The geometry of this steep zone at depth is constrained by the reflection data. Following migration of the northern segment of the southern traverse (Figs 12 and 9c), it is clear that the prominent north-dipping reflector (between 3 and 5 s) projects up to the Insubric Line. This result supports models which predict that the Insubric fault zone assumes a listric geometry at depth (see e.g. Heitzmann 1987b). The strong reflectivity of the Insubric Line is most likely produced from its concentrated zones of intense deformation characterized by banded mylonites and strong lithologic contrasts (e.g. pre-Triassic basement, marble zones, and tonalites of the Oligocene Bergell intrusion; *cf.* Heitzmann 1987a). The origins of the reflections are most likely related to similar features discussed above within the Penninic nappes. This comparison is appropriate since the Penninic nappes steepen into a belt just north of the Insubric Line (*cf.* Milnes 1974).

The successful imaging of the steeply-dipping Insubric

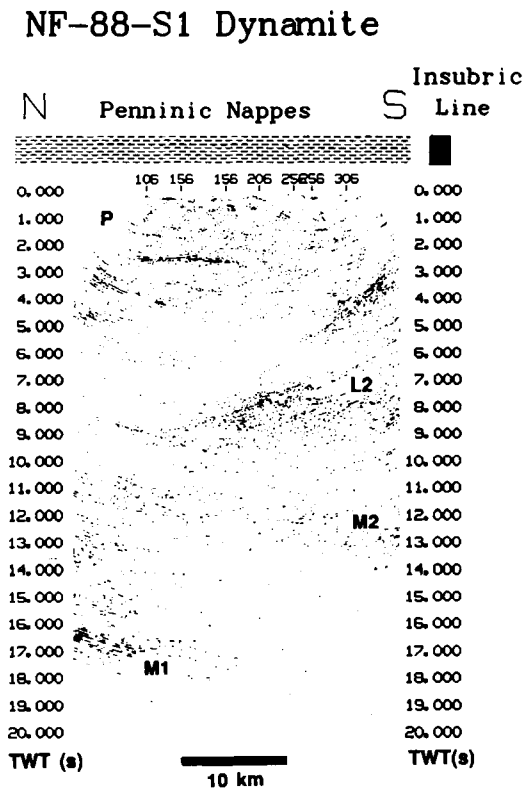

Figure 12. Migration of the northernmost profile S1 of the southern traverse (Fig. 6). A constant velocity (6 km s^{-1}) frequency–wavenumber migration was used. The surface trace of the Insubric fault zone is indicated in the upper right-hand corner of the section.

Line is largely due to the optimal source and receiver locations employed in the field. On the near-vertical incidence profile S3 (Figs 6 and 9) which crosses directly over its surface exposures, most of the energy reflected off the Insubric Line is defocused away from the profile. However, the northern location of profile S1 with respect to the Insubric Line was ideally suited for capturing its reflection.

South of the Insubric Line, the data quality across the Southern Alps decreases significantly. This is largely attributed to the high noise level and the poor coupling/transmission characteristics within this major transportation conduit between Switzerland and Italy. The sparse reflections which are imaged are interpreted as north-dipping basement wedges overriding the Mesozoic sediments. These basement slices are thought to have been backthrusted from locations beneath the Insubric Line (Heitzmann 1987b; Laubscher 1988; Roeder 1989). Further relationships between the Insubric Line and adjacent regions are discussed in the following sections.

Deep crust

The overall crustal structure revealed by the NFP 20 data supports earlier findings which indicated an asymmetrical thickening of the crust beneath the southern part of the Alps (Mueller *et al.* 1980). This over-thickened crust is expected to have developed as a consequence of several hundreds of kilometres of shortening during the continent–continent collision. A key to understanding how this mass was displaced and/or consumed is contained in the structural relationship between the European and Adriatic crustal plates. The NFP 20 reflection data (Figs 5 and 6) and the recent EGT refraction measurements (Fig. 9) provide an increased resolution which permits new insights into the present plate configuration. These new data document a zone of crustal indentation and subduction involving the descent of the European plate beneath the Adriatic microplate. The maximum crustal thickness is located in the vicinity of this juxtaposition which itself is laterally displaced south of the highest topography in the Alps.

The present relationship between the European and Adriatic crust is established through the integrated analysis of the EGT and NFP 20 reflection data. From the composite section (Fig. 9) the European and Adriatic crustal plates are defined by the *PmP* wide-angle reflected phase and the near-vertical incidence reflections M1 and M2, respectively. In this N–S profile across the Alps, the Adriatic microplate appears to have indented into the descending European plate.

The south-plunging European plate is also documented on fan recordings located east of the main profiles (Fig. 7). The successively deeper position of the Moho on these fans indicates a slight eastward component of dip. Earlier west–east refraction profiles in the Southern Alps (Deichmann, Ansorge & Mueller 1986) also show a gradual eastward thickening of the Adriatic crust. The observed apparent structuring in both the N–S and E–W directions outlines the 3-D nature of these crustal plates. Detailed investigations into the 2-D and 3-D effects on the seismic images are currently underway (Valasek & Holliger 1990). Here we have shown a conceptual, 2-D hand migration of the crustal boundaries which resolves a significant portion of the geometric distortion (Fig. 9c).

Deep structures north of the root zone

Reflections above the Moho north of the root zone may originate from processes that were active during the pre-collisional periods of crustal extension. These reflections (M1) occur in a 3–6 km thick zone beneath a less reflective area of the lower crust above the Moho (Figs 5 and 7). Data collected by NFP 20 along the western traverse (Valasek *et al.* 1990) and the ECORS–CROP profile in the western Alps (Bayer *et al.* 1987) show a similar band of reflections beneath the European foreland which indicates that this feature is laterally continuous throughout the Alpine arc. This reflection character can be compared to world-wide observations made in extensional environments (see e.g. Hale & Thompson 1982), such as the Basin and Range province of North America (Klemperer *et al.* 1986).

Heterogeneous reflection fabrics similar to M1 have been reproduced from models characterized by alternating high- and low-velocity layers (e.g. Wong, Smithson & Zawislak 1982; Deichmann & Ansorge 1983; Sandmeier & Wenzel 1986). Another study of relevance was carried out in the Ivrea Zone (Fountain 1986). During late Palaeozoic to early Mesozoic crustal extension (Brodie, Rex & Rutter 1989), the northern Adriatic margin presumably experienced metamorphism and underplating of mafic and ultramafic

material at the base of the crust. These deep-seated rocks were later uplifted to form the present Ivrea Zone exposures through a combined process of denudation (Schmid, Zingg & Handy 1987) followed by Alpine folding and tilting (Brodie & Rutter 1987; Handy 1987). Fountain (1986) found through synthetic modelling that the Ivrea exposures produce a band of layered reflections which distinguish the underplated regions from the poorly reflective, less mafic crust above. Prior to the closure of the Tethys, the southern European continental margin was also undergoing rift-related extension. Emplacement of magmatic material at the base of the crust during this period, in a process similar to that proposed for the Ivrea Zone, could have produced the deep reflection fabric observed in large areas of the present European foreland. In the Alps, the additional observation of the increase in low-frequency energy of the *PmP* phase relative to the high frequencies with increasing offset (offsets > 100 km, Fig. 9a) has been shown in other areas to result from attenuation or tunnelling as the waves propagate through a lamellar structure (e.g. in northern France, *cf.* Paul & Nicollin 1989). East–west refraction lines crossing the NFP 20 profiles show that this crustal transition zone (M1) is characterized by a sharp increase in velocity from 6.3 to 7.2 km s^{-1} (Maurer 1989). These velocities are in the range of those determined by laboratory measurements for mafic lithologies (Christensen 1982).

The lower crust (L1) north of the root zone is weakly defined on the seismic data (Figs 5 and 9). An E–W refraction profile crossing the northern margin of the Alps (Maurer 1989) shows a zone with an increase in seismic velocity from 6.3 to 6.6 km s^{-1} at a depth of about 24 km which coincides with the reflection L1. This high velocity probably represents an averaging of dominantly mafic rocks interlayered with felsic material. The lower crust seems to plunge southward paralleling the European Moho until it is lost within the root zone. From this geometry both the lower crust (L1) and Moho (M1) north of the root zone which are detached from the upper and middle crust appear to be relatively unaffected by Alpine deformation (Mueller 1990).

Deep structures within the root zone

A thickened crust is observed within the Alpine root zone beneath the Penninic nappes (Fig. 9). While prominent reflections define the fine details of the overlying nappes, the deeper crust demonstrates little reflectivity. This may in part be related to the higher degree of deformation experienced in this region during the Alpine orogeny. Determinations of the velocity structure in this region from the EGT and earlier seismic refraction data indicate that the deeper crust, extending from the Aar massif to the middle of the Penninic zone between 22 and 45 km, is characterized by rather low seismic velocities (Ottinger 1976; Yan & Mechie 1989). This implies that a large volume of this overthickened crust is dominated by silicic lithologies. Support for this is given by surface projections which show the external crystalline massifs plunging southward beneath the Penninic allochthon (Fig. 2, Trümpy 1985).

The detachment system responsible for the crustal doubling observed in the Alpine root zone is likely to be characterized by zones of concentrated (possibly mylonitic) deformation. If these zones have a low-angle geometry, then there is a stronger possibility that they would be detected on the seismic data; however, the NFP 20 data show little reflectivity beneath the Penninic nappes (Fig. 5a). One possibility for the lack of reflectivity is that the displacements may occur within a complex system of steep thrusts, as for example, postulated for the western Alps by Butler, Matthews & Parish (1986). Energy reflecting off the moderate contrasts between basement slices displaced within this system would be significantly defocused away from the near-vertical incidence recording array. Support for this suggestion arises from the observation that the only deep reflections recorded within the root zone occur on wide-angle measurements (e.g. line S1 in Figs 6 and 9, the DFSV spreads in Fig. 8, and the EGT data in Fig. 9: shot D→S at offsets from 210 to 290 km). The successful imaging of the steeply dipping deep reflections recorded on these profiles is a function of focusing made possible by optimal receiver–shot positioning with respect to the dipping structures.

Several other factors may also contribute to the low reflectivity of the deep crust within the root zone. On the near-vertical incidence data (Fig. 5) energy trapped within the strong acoustic impedance contrasts in the overlying Penninic zone may prevent imaging of weaker, more complex features below. The wide-angle recordings discussed above avoid this potential problem by undershooting the stack of Penninic nappes.

In addition, the transparent seismic response may in part be related to scattering generated from 3-D variations within the detachment system. The bias towards a 2-D construction from the N–S profiles may be misleading. It has been previously established that the crustal boundaries themselves are 3-D and it is well known, particularly from the western Alps, that E–W movements have occurred through the Alpine orogeny (*cf.* Laubscher 1989). The right-lateral movements of the Insubric Line and E–W strain indicators within the Penninic nappes point to significant lateral deformation within the central Alps (Merle, Cobbold & Schmid 1989). In this view, we propose that the crust has thickened by an anastomosing system of steep thrusts. The overall framework resembles an accretionary prism with its main detachment likely originating in the less viscous lower crust (Meissner 1989).

Crustal subduction and Adriatic indenter

The geometry of the European Moho (M1) within the root zone (Fig. 9) defines a crustal subduction zone. It reaches down to depths exceeding 60 km beneath the overriding Adriatic microplate. During collision, the crust has thickened during both northward transport and southward backthrusting while the lower crustal constituents are continually being displaced into the upper mantle. This is supported by evidence of a dense, high-velocity lithospheric slab descending southward beneath the Alps and the Po Plain (Mueller & Panza 1986; Spakman 1986; Mueller 1989). The ongoing crustal deformation may be in part propelled by the delamination of this unstable subcrustal slab as has been proposed for the Himalayas (Bird 1978).

The top of the Adriatic lower crust is defined by the reflection zone L2 in a position well north of its crustal

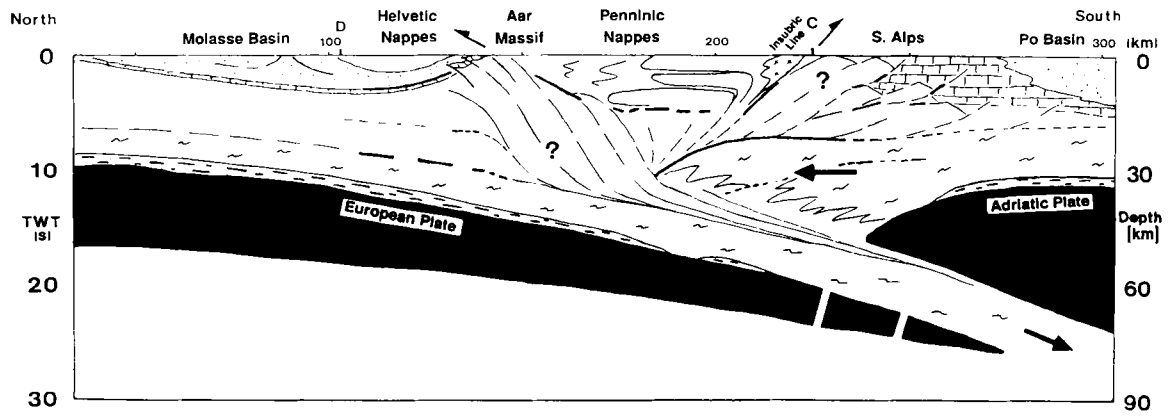

Figure 13. A schematic crustal cross-section showing the main features of the Alps and adjacent regions. This section is based on an integration of surface geologic information (e.g. Trümpy 1980; Pfiffner 1985; Schmid *et al.* 1989; Roeder 1989; Pfiffner *et al.* 1990b) and the combination of the NFP 20 and EGT seismic reflection data. The heavy lines represent the main crustal reflections migrated in Fig. 9(c). Refer to text for a detailed explanation.

boundary M2 (Figs 6 and 9). This zone has a geometry which parallels the base of the Adriatic microplate, and together they define a major crustal indenter penetrating beneath the Penninic allochthon and above the subducting European foreland (Frei *et al.* 1989). This wedging-subduction process appears to be responsible for shortening and thickening the crust along a steep array of north-vergent thrusts and southward backthrusting (*cf.* Fig. 13).

Comparison to the ECORS–CROP western Alps profile

The results of the ECORS–CROP deep-crustal reflection measurements across the western Alps (Bayer *et al.* 1987) show striking similarities to the findings made further east across the Swiss Alps. In particular, the subsurface images of the upper crustal structures (Helvetic and Penninic domains) could almost be interchanged. The overall structure in the western Alps has been interpreted as being developed by a similar process of crustal wedging and subduction (Butler *et al.* 1986; Nicolas *et al.* 1990). These findings, particularly the relationship between the crustal plates, were largely supported by additional data such as those from gravity measurements and seismic fan recordings. In the central Alps, the extent of the crustal plates defined by the seismic reflection data alone are sufficient enough to lead us to an interpretation.

The primary difference between the two data sets is that in the central Alps only one crustal indenter has been clearly identified, whereas to the west, the southern plate appears to be imbricated into at least two wedges, one of them residing beneath the Ivrea Zone. In addition, the geometry of these imbrications varies with more inclined crustal slices in the western Alps than in the east (Coward & Dietrich 1989). The more simplified situation in the central Alps, may be explained by the lack of a rigid intracrustal feature such as the high-density Ivrea body. The Ivrea body lacks significant internal deformation which may be explained by the presence of upper mantle and lower crustal material, such as olivine and feldspar which is more resistant to hardening than quartz at shallow levels (Schmid *et al.* 1989). During collision in the western Alps, the intracrustal position of the Ivrea body may have acted as a buttress which transferred stress into more frontal regions ultimately leading to the development of additional crustal imbrications.

A larger amount of total crustal shortening in the western Alps compared to the central Alps also supports the apparent higher degree of crustal imbrication in the western Alps. Westward motion of the Adriatic plate in response to E–W directed Tertiary shortening of over 300 km has been postulated for the western Alps (Laubscher 1984). This may be manifested by the presence of significant horizontal velocity variations which indicates that crustal interfingering was more intense in the internal structure of the western Alps than in the central Alps (Miller, Mueller & Perrier 1982).

6 CONCLUSIONS

The initial results of seismic reflection profiling across the central Alps of eastern Switzerland provide new insights into the present structure and past evolution of this continent–continent collision zone. The findings are summarized in a schematic N–S cross-section extending across the Alps (Fig. 13).

The present crustal structure appears to contain elements which document several phases of deformation. Evidence for extensional deformation prior to collision is preserved adjacent to the Alpine root zone in the lowermost crust of the European foreland. A heterogeneous crust–mantle transition zone which developed during pre-Alpine extension is interpreted to be represented by a passive marker consisting of a band of layered reflections above the present European Moho.

More recent Alpine compression has reshaped most of the remaining crustal structure. The present crustal framework appears to document a northward indentation of the Adriatic microplate into the European continent. This resulted in detachments at several crustal levels with both northward telescoping of basement slices (as e.g. the Aar and Gotthard Massifs) and south-vergent backthrusting in the Southern Alps. During this process, lower crustal material within the root zone has been displaced into the upper mantle.

While significant crustal doubling is observed, the system responsible for the stacking and displacement of the crust is

not well resolved by the reflection data. This is interpreted to indicate a complex detachment system which resembles an accretionary wedge of crustal slabs. A sole thrust originating from the top of the lower crust is tentatively interpreted to have carried the external basement slices up through a complex array of thrusts.

At shallower crustal levels, the Alpine deformation is better documented by the reflection data. In particular, prominent reflections define the overall structure of the Penninic allochthon displaced during early stages of collision onto the European continent. The older internal geometry of this collapsed basinal sequence is outlined by strong reflections that are produced from zones of intense ductile deformation and compositional variations. The subsurface geometry of the more recent bounding fault zones, the basal thrust of the Penninic nappes to the north (P.F. in Fig. 2) and the Insubric Line to the south are clearly imaged in the subsurface. This asymmetric 'pop-up' structure is mobilized by north-vergent thrusting and south-directed backthrusting which is controlled by the wedging Adriatic microplate. This supports earlier suggestions that the Penninic domain forms an asymmetric wedge completely detached from the crust below (Laubscher 1983; Schmid *et al.* 1989).

In general, the data show strong similarities with the recent deep-crustal investigations across the western Alps (Nicolas *et al.* 1990). Both data sets consistently show a doubling of the crust by indentation of the southern plate and subduction of the European foreland. However, the influence of the Ivrea body together with greater overall shortening in the western Alps has acted as a buttress and led to more complicated crustal imbrications than in the central Alps.

ACKNOWLEDGMENTS

Primary funding for this project was provided by the Swiss National Science Foundation through the special support of the National Research Program 20 'Deep Geological Structure of Switzerland'. The cooperative efforts together with CROP-Italia were instrumental in extending our observations across key areas of the Alps. The authors would like to thank the numerous colleagues and students who helped throughout the various stages of this project. In particular, Peter Finckh is acknowledged for his work in establishing the data processing centre and in leading the DFS V data acquisition team. The project benefited considerably from the assistance of Scott Smithson and other collaborators from the University of Wyoming who were supported by US National Science Foundation grants EAR-8300659 and EAR-8419154. Critical evaluations by Scott Smithson, Adrian Pfiffner and two anonymous reviewers helped substantially to improve this paper. Contribution no. 642, ETH Geophysics, Zürich, Switzerland.

REFERENCES

Barton, P. J., 1986. Comparison of deep reflection and refraction structures in the North Sea, in *Reflection Seismology: A Global Perspective,* vol. 13, pp. 279–300, eds Barazangi, M. & Brown, L., Geodynamics Series of the American Geophysical Union, Washington, DC.

Bayer, R. *et al.*, 1987. Premiers résultats d'une traversée des Alpes occidentales par sismique réflexion verticale (Programme ECORS–CROP), *C.R. Acad. Sci. Paris,* **305 II,** 1461–1470.

Bird, P., 1978. Initiation of intracontinental subduction in the Himalaya, *J. geophys. Res.*, **83,** 4975–4987.

Brodie, K. H. & Rutter, E. H., 1987. Deep crustal extensional faulting in the Ivrea zone of northern Italy, *Tectonophysics,* **140,** 193–212.

Brodie, K. H., Rex, D. & Rutter, E. H., 1989. On the age of deep crustal extensional faulting in the Ivrea zone, northern Italy, in *Alpine Tectonics,* vol. 45, pp. 203–210, eds Coward, M. P., Dietrich, D. & Park, R. G., Special Publication of the Geological Society of London.

Buness, H., Giese, P., Hirn, A., Nadir, S. & Scarascia, S., 1990. Crustal structure derived from seismic refraction between the Southern Alps and the Ligurian Sea, in *Sixth EGT Workshop—Data Compilations and Synoptic Interpretation,* pp. 165–168, eds Freeman, R. & Mueller, St., European Science Foundation, Strasbourg.

Butler, R. W. H., Matthews, S. J. & Parish, M., 1986. The NW external Alpine thrust belt and its implications for the geometry of the western Alpine orogen, in *Collision Tectonics,* vol. 19, pp. 245–260, eds Coward, M. P. & Ries, A. C., Special Publication of the Geological Society of London.

Christensen, N. I., 1982. Seismic velocities, in *Handbook of Physical Properties,* pp. 1–228, ed. Carmichael, R. S., CRC Press, Boca Raton.

Christensen, N. I. & Szymanski, D. L., 1988. Origin of reflections from the Brevard Fault Zone, *J. geophys. Res.*, **93,** 1087–1102.

Coruh, C. & Costain, J., 1983. Noise attenuation by Vibroseis whitening (VSW) processing, *Geophysics,* **48,** 543–554.

Coward, M. & Dietrich, D., 1989. Alpine tectonics—an overview, in *Alpine Tectonics,* vol. 45, pp. 1–32, eds Coward, M. P., Dietrich, D. & Park, R. G., Special Publication of the Geological Society of London.

Dewey, J. F., Pitman, W. C. III, Ryan, W. B. F. & Bonnin, J., 1973. Plate tectonics and the evolution of the Alpine system, *Geol. Soc. Am. Bull.*, **84,** 3137–3180.

Dewey, J. F., Helman, M. L., Turco, F., Hutton, D. H. W. & Knott, S. D., 1989. Kinematics of the western Mediterranean, in *Alpine Tectonics,* vol. 45, pp. 265–283, eds Coward, M. P., Dietrich, D. & Park, R. G., Special Publication of the Geological Society of London.

Deichmann, N. & Ansorge, J., 1983. Evidence for lamination in the lower crust beneath the Black Forest (Southwest Germany), *J. Geophys.*, **52,** 109–118.

Deichmann, N., Ansorge, J. & Mueller, St., 1986. Crustal structure of the Southern Alps beneath the intersection with the European Geotraverse, *Tectonophysics,* **126,** 57–83.

EUGEMI Working Group, 1990. The European Geotraverse seismic refraction experiment of 1986 from Genova, Italy to Kiel, Germany, *Tectonophysics,* **176,** 43–58.

Frei, W., Heitzmann, P., Lehner, P., Mueller, St., Olivier, R., Pfiffner, A., Steck, A. & Valasek, P., 1989. Geotraverses across the Swiss Alps, *Nature,* **340,** 544–548.

Frey, M., Bucher, K., Frank, E. & Mullis, J., 1980. Alpine metamorphism along the Geotraverse Basel-Chiasso: a review, *Eclogae Geol. Helv.*, **73,** 527–546.

Frey, M., Hunziker, J. C., Frank, W., Bocquet, J., Dal Piaz, G. V., Jaeger, E. & Niggli, E., 1974. Alpine metamorphism of the Alps, *Schweiz. Min. Petr. Mitt.*, **54,** 247–290.

Fountain, D. M., 1986. Implications of deep crustal evolution for seismic reflection interpretation, in *Reflection Seismology: The Continental Crust,* vol. 14, pp. 1–8, eds Barazangi, M. & Brown, L., Geodynamics Series of the American Geophysical Union, Washington, DC.

Fountain, D. M., Hurich, C. A., & Smithson, S. B., 1984. Seismic reflectivity of mylonite zones in the crust, *Geology,* **12,** 195–198.

Gansser, A., 1968. The Insubric Line, a major geotectonic problem, *Schweiz. Min. Petr. Mitt.*, **48,** 123–143.

Hale, L. D. & Thompson, G. A., 1982. The seismic reflection character of the continental Mohorovičić discontinuity, *J. geophys. Res.*, **87,** 4625–4635.

Handy, M., 1987. The structure, age and kinematics of the Pogallo Fault zone: southern Alps, northwestern Italy, *Eclogae Geol. Helv.*, **80,** 593–632.

Heitzmann, P., 1987a. Calcite mylonites in the central Alpine 'root zone', *Tectonophysics,* **135,** 207–215.

Heitzmann, P., 1987b. Evidence of late Oligocene/Early Miocene backthrusting in the central Alpine 'root zone', *Geodinamica Acta,* **1,** 183–192.

Hirn, A., Nadir, S., Thouvenot, F., Nicolich, R., Pellis, G., Scarascia, S., Tabacco, I., Castellano, F. & Merlanti, F., 1989. Mapping the Moho of the Western Alps by wide-angle reflection seismics, *Tectonophysics,* **162,** 193–202.

Hurich, C. A. & Smithson, S. B., 1987. Compositional variation and origin of deep crustal reflections, *Earth planet. Sci. Lett.*, **85,** 416–426.

Hurford, A. J., Flisch, M. & Jäger, E., 1989. Unravelling the thermo-tectonic evolution of the Alps: a contribution from fission track analysis and mica dating, in *Alpine Tectonics,* vol. 45, pp. 369–398, eds Coward, M. P., Dietrich, D. & Park, R. G., Special Publication of the Geological Society of London.

Hurich, C. A., Smithson, S. B., Fountain, D. M., & Humphreys, M. C., 1985. Seismic evidence of mylonite reflectivity and deep structures in the Kettle dome metamorphic core complex, Washington, *Geology,* **13,** 577–580.

Kissling, E., Mueller, St. & Werner, D., 1983. Gravity anomalies, seismic structure and geothermal history of the Central Alps, *Annales Geophysicae,* **1,** 37–46.

Klemperer, S. L., Hauge, T. A., Hauser, E. C., Oliver, J. E. & Potter, C. J., 1986. The Moho in the northern Basin and Range province, Nevada, along the COCORP 40°N seismic-reflection transect, *Geol. Soc. Am. Bull.*, **97,** 603–618.

Laubscher, H. P., 1970. Bewegung und Wärme in der alpinen Orogenese, *Schweiz. Min. Petr. Mitt.*, **50,** 565–596.

Laubscher, H. P., 1974. The tectonics of subduction in the Alpine system, *Memorie della Societa Geologica Italiana,* **XIII,** Suppl. 2, 275–283.

Laubscher, H. P., 1983. Detachment, shear and compression in the central Alps, *Geol. Soc. Am. Mem.*, **158,** 191–211.

Laubscher, H. P., 1984. The tectonic problem of the Ivrea Body and the Insubric Line, *Annales Geophysicae,* **2,** 169–170.

Laubscher, H. P., 1988. Material balance in Alpine orogeny, *Geol. Soc. Am. Bull.*, **100,** 1313–1328.

Laubscher, H. P., 1989. The tectonics of the southern Alps and the Austro-Alpine nappes: a comparison, in *Alpine Tectonics,* vol. 45, pp. 229–242, eds Coward, M. P., Dietrich, D. & Park, R. G., Special Publication of the Geological Society of London.

Maurer, H. R., 1989. Die Struktur der Erdkruste unter dem schweizerischen Alpennordrand, *Diploma thesis,* ETH Zürich.

Meissner, R., 1989. Rupture, creep, lamellae and crocodiles: happenings in the continental crust, *Terra Nova,* **1,** 17–28.

Mereu, R. F., 1990. The complexity of the crust from refraction/wide-angle reflection data, *Pageoph,* **132,** 269–288.

Merle, O., Cobbold, P. R. & Schmid, S., 1989. Tertiary kinematics in the Lepontine dome, in *Alpine Tectonics,* vol. 45, pp. 113–134, eds Coward, M. P., Dietrich, D. & Park, R. G., Special Publication of the Geological Society of London.

Miller, H., Mueller, St. & Perrier, G., 1982. Structure and dynamics of the Alps—a geophysical inventory, in *Alpine–Mediterranean Geodynamics,* vol. 7, pp. 175–203, eds Berckhemer, H. & Hsü, K. J., Geodynamics Series of the American Geophysical Union, Washington, DC.

Milnes, A. G., 1974. Structure of the Penninic zone (central Alps): a new working hypothesis, *Geol. Soc. Am. Bull.*, **85,** 1725–1732.

Mueller, St., 1989. Deep-reaching geodynamic processes in the Alps, in *Alpine Tectonics,* vol. 45, pp. 303–328, eds Coward, M. P., Dietrch, D. & Park, R. G., Special Publication of the Geological Society of London.

Mueller, St., 1990. Intracrustal detachment and wedging along a detailed cross-section in Central Europe, in *Exposed Cross-Sections of the Continental Crust.* pp. 623–643, eds Salisbury, M. H. & Fountain, D. M., Kluwer, Dordrecht.

Mueller, St., 1990. Intracrustal detachment and wedging along a detailed cross-section in Central Europe, in *Exposed Cross-Sections of the Continental Crust,* eds Salisbury, M. H. & Fountain, D. M., Kluwer, Dordrecht, in press.

Mueller, St. & Banda, E., 1983. The European Geotraverse Project, *Terra Cognita,* **3,** 291–294.

Mueller, St. & Panza, G. F., 1986. Evidence of a deep-reaching lithospheric root under the Alpine arc, in *The Origin of Arcs,* vol. 21, pp. 93–113, ed. Wezel, F. C., Developments in Geotectonics, Elsevier, Amsterdam.

Mueller, St., Ansorge, J., Egloff, R. & Kissling, E., 1980. A crustal cross section along the Swiss Geotraverse from the Rhinegraben to the Po Plain, *Eclogae Geol. Helv.*, **73,** 463–483.

Nicolas, A., Hirn, A., Nicolich, R., Polino, R. & the ECORS–CROP Working Group, 1990. Lithospheric wedging in the western Alps inferred from the ECORS–CROP traverse, *Geology,* **18,** 587–590.

Ottinger, T., 1976. Der Aufbau der Erdkruste unter dem Schweizerischen Teil des Refraktionsseismischen Alpenlängsprofils von 1975, *Diploma thesis,* ETH Zürich.

Paul, A. & Nicollin, F., 1989. Thin crustal layering in Northern France: observations and modelling of the *PmP* spectral content, *Geophys. J. Int.*, **99,** 229–246.

Pfiffner, O. A., 1985. Displacements along thrust faults, *Eclogae Geol. Helv.*, **78,** 313–333.

Pfiffner, O. A., Frei, W., Finckh, P. & Valasek, P., 1988. Deep seismic reflection profiling in the Swiss Alps: Explosion seismology results for line NFP 20-EAST, *Geology,* **16,** 987–990.

Pfiffner, O. A., Klaper, E. M., Mayerat, A. M. & Heitzmann, P., 1990a. Structure of the basement-cover contact in the Swiss Alps, in *Deep Structure of the Alps,* eds Roure, F., Heitzmann, P. & Polino, R., Mém. géol. Soc. France, 155, Mém. Soc. Géol. Suisse, 1, Soc. geol. Ital., Vol. spec. 1, in press.

Pfiffner, O. A., Frei, W., Valasek, P., Stäuble, M., DuBois, L., Levato, L., Schmid, S. & Smithson, S. B., 1990b. Crustal shortening in the Alpine orogen: results from deep seismic reflection profiling in the eastern Swiss Alps—line NFP 20-EAST, *Tectonics,* **9,** 1327–1356.

Roeder, D., 1989. South-Alpine thrusting and trans-Alpine convergence, in *Alpine Tectonics,* vol. 45, pp. 211–228, eds Coward, M. P., Dietrich, D. & Park, R. G., Special Publication of the Geological Society of London.

Sandmeier, K. J. & Wenzel, F., 1986. Synthetic seismograms for a complex model, *Geophys. Res. Lett.*, **13,** 22–25.

Schmid, S. M., Zingg, A. & Handy, M., 1987. The kinematics of movement along the Insubric Line and the emplacement of the Ivrea Zone, *Tectonophysics,* **135,** 47–66.

Schmid, S. M., Aebli, H. R., Heller, F. & Zingg, A., 1989. The role of the Periadriatic Line in the tectonic evolution of the Alps, in *Alpine Tectonics,* vol. 45, pp. 153–171, eds Coward, M. P., Dietrich, D. & Park, R. G., Special Publication of the Geological Society of London.

Spakman, W., 1986. The upper mantle structure in the central European–Mediterranean region, in *Third EGT Workshop—The Central Segment,* pp. 215–221, eds Freeman, R., Mueller, St. & Giese, P., European Science Foundation, Strasbourg.

Stanley, P. J., 1986. Some comments regarding ambient noise in Vibroseis surveys, *First Break*, **4**, 31–33.

Stäuble, M., 1990. Seismic reflection profiling from the Molasse Basin into the Alps of eastern Switzerland: processing, interpretation and modelling, *PhD thesis*, University of Berne.

Trümpy, R., 1980. *Geology of Switzerland—a Guide Book*, Wepf. & Co., New York.

Trümpy, R., 1985. Die Plattentektonik und die Entstehung der Alpen, *Neujahrsblatt Naturforsch. Ges. Zürich*, **187**, 1–47.

Valasek, P. & Holliger, K., 1990. Approaches towards an integrated interpretation of the NFP 20 deep crustal reflection profiles along the Alpine segment of the EGT, in *Sixth EGT Workshop—Data Compilations and Synoptic Interpretation*, pp. 137–148, eds Freeman, R. & Mueller, St., European Science Foundation, Strasbourg.

Valasek, P. A., Snoke, A. W., Hurich, C. A., & Smithson, S. B., 1989. Nature and origin of seismic reflection fabric, Ruby-East Humboldt metamorphic core complex, Nevada, *Tectonics*, **8**, 391–415.

Valasek, P., Frei, W., Stäuble, M. & Holliger, K., 1990. Processing of the NFP 20 seismic reflection traverses across the Swiss Alps by the ETH Zürich data processing center, in *Deep Structure of the Alps*, eds Roure, F., Heitzmann, P. & Polino, R., Mém. géol. Soc. France, 155, Mém. Soc. Géol. Suisse, 1, Soc. geol. Ital., Vol. spec. 1, in press.

Wong, Y. K., Smithson, S. B. & Zawislak, R. L., 1982. The role of seismic modeling in deep crustal reflection interpretation, Part 1, *Contrib. Geol.*, **20**, 91–109.

Yan, Q. Z. & Mechie, J., 1989. A fine structural section through the crust and lower lithosphere along the axial region of the Alps, *Geophys. J. Int.*, **98**, 465–488.

Ye, S. & Ansorge, J., 1990. The compilation of deep seismic refraction data along the EGT main profile between the Danube River and the Gulf of Genova, in *Sixth EGT Workshop—Data Compilations and Synoptic Interpretation*, pp. 129–136, eds Freeman, R. & Mueller, St., European Science Foundation, Strasbourg.